ISSN 1392–1320 MATERIALS SCIENCE (MEDŽIAGOTYRA). Vol. XX, No. X. 2023

Effect of Lateral Load on Local Buckling of Latex Wrapped Cold Formed Steel Columns

Rajivgandhi NARASIMHAN *, Jane Helena HENDERSON

Department of Civil Engineering, College of Engineering, Guindy, Anna University, Chennai 600 025, India

crossref http://dx.doi.org/10.5755/j02.ms.31876

Received 22 July 2022; accepted 26 October 2022

This paper reports the experimental investigation conducted on unwrapped and latex wrapped cold-formed steel column. Various column cross-sections are subjected to repeated lateral loading till failure. All the columns were observed to fail in local buckling. The column cross-section dimension, provision of interior and exterior lip, and the latex wrapping of the columns influenced the lateral load to failure. Increasing the web length of a column section from 100 to 200 mm increased the load-carrying capacity of the column by 70 to 100 %. The local buckling was initiated in the flange portion of the column. The column section with no lip and interior lip exhibited inward buckling of the flange. The column with exterior lip exhibited outward buckling. The provision of lip and latex wrapping did not influence the initial load-displacement behavior of the columns. However, it increased the load-carrying capacity of the sections. Energy absorption index and ductility factor were calculated and the effect of latex wrapping of the columns on these parameters was evident.

Keywords: cold formed steel column, lateral buckling, channel section, back-to-back channel section, latex wrapping, energy absorption index.

1. INTRODUCTION

Cold Form Steel (CFS) columns are currently used in lightweight framed structures. Extensive research has been conducted globally to understand the behaviour of CFS columns subjected to axial loading [1 – 3]. However, there is only limited research available on the understanding of the behaviour of CFS columns subjected to lateral loading [4]. In this investigation, an attempt has been made to understand the behaviour of CFS columns to lateral loading.

CFS column sections are more prone to buckling and the buckling can be local, distortional and global or the interaction of all three [5]. Euro code [6] recommends the following design constrain to avoid buckling in the CFS column: the ratio of gross width to plate thickness is recommended to be less than or equal to 60; the ratio of lip width to thickness is restricted to 50; the ratio of web height to thickness is restricted to 500; the lip width to cross-section width is kept in the range of 0.2 to 0.6. New cross-sections can be designed by considering the above recommendations. The ultimate load carrying capacity is expected to depend on the cross-section of the CFS column and the end conditions. Young et al., [7 – 9] experimentally determined the ultimate axial load capacity of plain and lipped CFS channel section. The experiment was conducted with pinned and fixed end boundary conditions. The centroid was observed to be shifted due to local buckling.

When the CFS column is subjected to axial load, Weng, 1991 [10] showed that the column yields from the inside surface and the yield zone were observed to propagate as the loading increases. Hence, the plate thickness that is initially effective reduces on loading. Further, standards recommend the effective width concept in the design of compression member for local buckling [11]. There is a good understanding of the effective width of the CFS column on the axial load, however, the influence of lateral loading on the effective width of the column is not commonly known.

The strengthening of a member can be achieved either by bracing or by wrapping the structural member with light weight laminates. These methods are proved to be successful in improving the buckling strength of the member [12 – 16]. Anbarasu et al., 2015 used a V-type stiffener to strengthen the web and prevent local buckling at the web of the CFS column. Kherbouche et al., 2019 and Dar et al., 2021 showed that cross-section design influenced the buckling failure of the CFS columns [13, 14]. Closed cross-sections perform better when compared to open cross-sections. Naganathan et al., 2020, conducted an experimental investigation on CFS columns wrapped with carbon fibre reinforced polymer and observed that wrapping strengthened and delayed the local buckling that occurred in the CFS column [15]. Dar, 2021, reinforced the CFS column using glass fiber reinforced polymer planks and it was experimentally observed that reinforcement improved the axial load capacity and delayed the local buckling [16]. Baabu et al., 2017 used glass fiber reinforced polymer (GFRP) to wrap the CFS column section [17]. GFRP wrapped CFS column section was tested under axial loading and load carrying capacity of the column was found to increase up to 80%. The strengthening of the CFS column using any kind of sheathing is expected to increase the effective thickness of the column and hence increase the load carrying capacity of the structural element. The natural latex that is found in abundance can be considered as one of the options for reinforcement for the CFS column. While most of the

* Corresponding author. Tel.: +91- 9677118112
E-mail address: *rajivgandhi.n.civil@psvpec.in* (N.Rajivgandhi)

experimental study was conducted to understand the characteristic behaviour of CFS columns under axial loading, the behaviour of wrapped CFS column sections under lateral loading is not been analyzed to the required rigour.

To understand the behaviour of the CFS column to lateral and cyclic loading, the parameters viz. its load carrying capacity, stiffness, ductility factor and energy absorption index are considered. These factors define the extent of deformation the particular structural member can undergo before it fails. The latex wrapped CFS column is expected to exhibit a better ductility factor when compared to the unwrapped column. Gajalakshmi and Helena, 2012 used concrete ductility factor and energy absorption parameters for the study of concrete infilled column [18]. The ductility factory is defined as the ratio of the displacement corresponding to the maximum lateral load to displacement at which the first yield or local buckling occurs [18, 19]. The energy absorption loading is measured from the area enclosed within the load-displacement curve. The stiffness of the column, which is defined as the ratio of peak lateral force to the corresponding displacement during cyclic loading is expected to decrease as the column develops failure during repeated loading. El-Taly et al., 2020 used ductility factor, energy absorption and stiffness to optimize the cross-section of the CFS column to lateral loading.

The main objective of this paper is to understand the behaviour of CFS columns when subjected to lateral loading. CFS channel and back-to-back cross-section with different web lengths were subjected to lateral loading. The influence of lip to buckling of the CFS columns is reported. All the CFS columns are also strengthened using latex wrapping and their lateral displacement and local buckling behaviour are studied. The ductility factor, stiffness and energy absorption index are estimated for all the conditions and the influence of cross-section, lip and latex wrapping in the CFS column are estimated.

2. EXPERIMENTAL INVESTIGATION

2.1. Materials

Cold form steel sheet of 2 mm is used for column fabrication. The yield point of the steel sheet and the ultimate tensile strength was tested following IS8811, 1998. The yield point of the steel sheet was observed as 237 MPa and the ultimate tensile strength was 331 MPa.

The natural latex sheet of 3mm thick as shown in Fig. 1 is used for wrapping the steel section. The tensile strength of the latex sheet when tested following ASTM D412-16, 2021 is observed to be 1.46 MPa and the elongation is 112.63 %, which is nearly four times that of the steel sheet.

2.2. Specimen fabrication

Twelve different column sections with two sets in each section were fabricated using the steel sheet. One set of columns was tested in unwrapped conditions and the other set was tested after wrapping the column with the latex sheet (Fig. 1).

Fig. 1. Image of latex sheet used for wrapping the column

The cross-section details and the sample designation of each column in unwrapped conditions are shown in Fig. 2. Two sizes of channel sections (100 × 50 × 2 mm and 200 × 50 × 2 mm) were used.

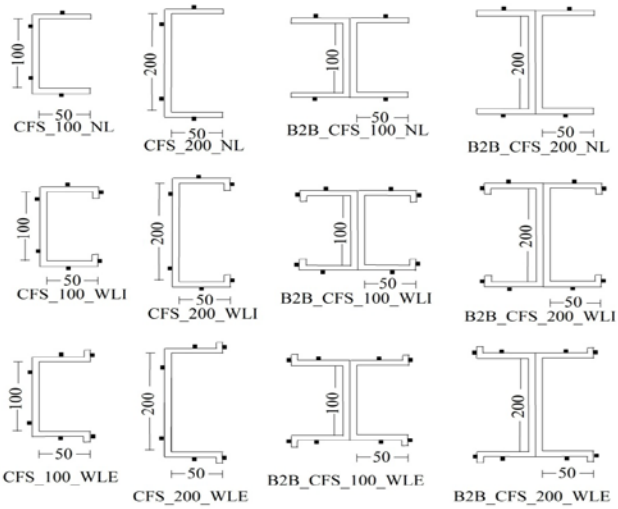

Fig. 2. Cross-section details of unwrapped columns with sample designation

Six-channel sections with and without a lip and six back-to-back channel sections with and without a lip were tested. The cross-sections are differentiated based on the longer dimension of the section (100 and 200 mm), and the provision of the lip. The sections are fabricated without a lip, with an interior lip of 12 mm, and with an exterior lip of 12 mm. Further, the latex sheet is glued to one set of column sections, and a total of 24 different column sections with and without latex wrapping are tested. The unwrapped channel sections without lip are designated as CFS_100_NL and CFS_200_NL. The unwrapped channel sections with an interior lip are designated as CFS_100_WLI and CFS_200_WLI. The unwrapped channel sections with exterior lip are designated as CFS_100_WLE and CFS_200_WLE. The back-to-back channels are designated as B2B_CFS_100_NL, B2B_CFS_200_NL, B2B_CFS_100_WLI, B2B_CFS_200_WLI, B2B_CFS_100_WLE, and B2B_CFS_200_WLE. The latex wrapped sections with no lip are designated as CFS_100_NL_RW, CFS_200_NL_RW, B2B_CFS_100_NL_RW, and

B2B_CFS_200_NL_RW. The latex wrapped sections with interior lip are designated as CFS_100_WLI_RW, CFS_200_WLI_RW, B2B_CFS_100_WLI_RW, and B2B_CFS_200_WLI_RW. The latex wrapped sections with exterior lip are designated as CFS_100_WLE_RW, CFS_200_WLE_RW, B2B_CFS_100_WLE_RW, and B2B_CFS_200_WLE_RW. The height of the column is kept at 1.25 m.

The height of the column is ensured to be greater than three times the largest dimension and less than 20 times the radius of gyration determined about the weak axis. All the columns are welded to the base plate of size 300 × 300 × 12 mm. During welding, the centroid of the column section is made to coincide with the centroid of the plate. Fig. 3 shows all 24 fabricated samples before testing.

Fig. 3. Wrapped and unwrapped columns before testing

2.3. Test protocol

Each column section is simultaneously subjected to constant axial load and repeated cycles of lateral load. The magnitude of axial load is determined from the theoretically calculated ultimate load following IS801, 1975. All column sections are subjected to an axial load of magnitude equal to one-tenth of the ultimate load determined for the unwrapped section. The axial load of the wrapped section is kept the same as that of the unwrapped specimen. The axial load is applied at the centroid of the column. Table 1 shows the ultimate load to failure and the applied axial load for the specimens tested. In addition to the axial load, the specimens are also subjected to repeated lateral load. Fig. 4 a shows the experimental setup. The repeated lateral load is applied at the top of the column. Initially, a lateral load of 1 kN is applied to push the column toward the right from the neutral position. The lateral load in the column is released and the load of -1 kN is applied to push the sample to the left from the neutral position and then unloaded. This constitutes one cycle of loading. Further, the column is subjected to repeated loading, with lateral load incremented by 1 kN for every cycle. The schematic of the lateral load application is shown in Fig. 4 b. This repeated loading with a 1 kN load increment in each cycle is applied till the specimen fails. The lateral displacement near the free end of the column is measured for each cycle. To measure the strain in the local buckling zone, strain gauges are placed at 100 mm from the base plate. Four to eight gauges were used for different sections. The location of the strain gauges is indicated in Fig. 2.

Table 1. Theoretically computed ultimate load and the applied axial load for different specimens

No.	Sample	Ultimate load to failure, kN	Axial load applied, kN
1	CFS_100_NL and CFS_100_NL_RW	51.30	5
2	CFS_100_WLI, CFS_100_WLI_RW, CFS_100_WLE and CFS_100_WLE_RW	75.01	7
3	CFS_200_NL and CFS_200_NL_RW	65.86	6
4	CFS_200_WLI, CFS_200_WLI_RW, CFS_200_WLE and CFS_200_WLE_RW	87.15	7
5	B2B_CFS_100_NL and B2B_CFS_100_NL_RW	99.42	9
6	B2B_CFS_100_WLI, B2B_CFS_100_WLI_RW, B2B_CFS_100_WLE and B2B_CFS_100_WLE_RW	141.02	10
7	B2B_CFS_200_NL and B2B_CFS_200_NL_RW	135.77	10
8	B2B_CFS_200_WLI, B2B_CFS_200_WLI_RW, B2B_CFS_200_WLE and B2B_CFS_200_WLE_RW	174.33	10

a

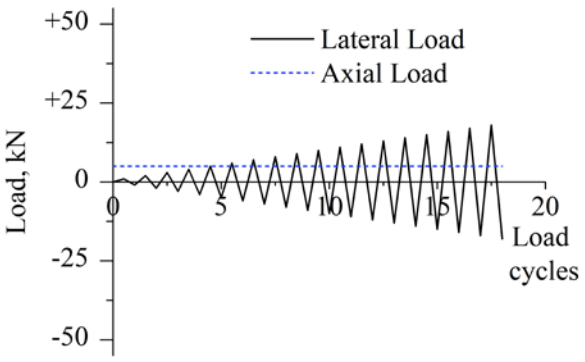

b

Fig. 4. Details of experimental investigation: a – experimental setup; b – schematic of load application

3. RESULTS AND DISCUSSION

3.1. Lateral load-lateral displacement at the free end of the column

The lateral displacement recorded at the free end of the column for different column sections was compared. Fig. 5 shows the load-displacement curve for column and back-to-back column sections without a lip. As expected, the cross-section of the column influences the load-displacement behaviour. Imran et al., 2018 [21] observed the web height to flange width ratio, which is defined as an aspect ratio to be an important parameter to control the local buckling. In this current investigation, the increase in web length from 100 to 200 mm reduced the lateral displacement by 30 to 40 %. The load corresponding to the lateral displacement was also increased when the web length was increased from 100 to 200 mm. The increase in lateral load was found to be 75 to 100 %.

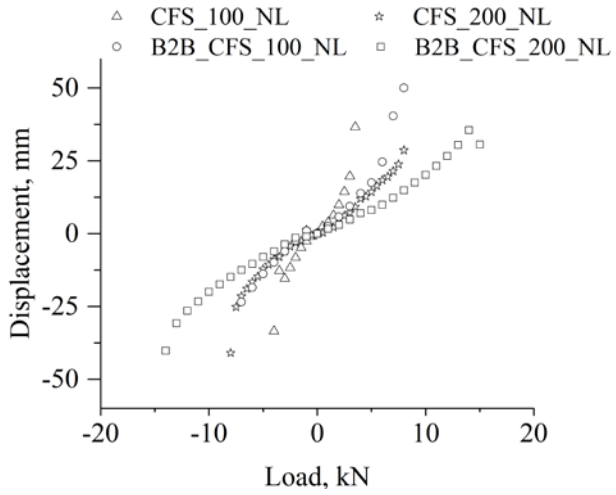

Fig. 5. Load-displacement curves of channel and back-to-back channel section without a lip

For any given cross-section the provision of the lip has increased the maximum load to failure. The load-displacement curve of the sections with exterior lip and without lip is shown in Fig. 6.

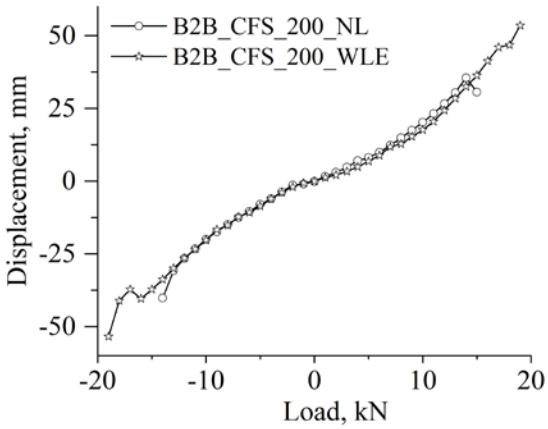

Fig. 6. Load-displacement curves of back-to-back channel section with and without a lip

The slope of the load-displacement curve remained the same for both B2B_CFS_200_NL and B2B_CFS_200_WLE. However, the maximum load to failure for the specimen that is with lip was found to be 5.0 kN. This is a 50 % increase when compared to the specimen without a lip. A similar trend was observed in all the cases of the channel and back-to-back channel sections with interior and exterior lips. Schafer, 2014 [22] observed that the provision of the lip in the angle section enchanced the buckling load in torsion-flexural modes. In the current investigation, the provision of lip (both interior and exterior), increased the ultimate load and the increase was in the range of 40 to 50 %.

The influence of latex wrapping on the lateral displacement of the specimen is shown in Fig. 7. Fig. 7 a compares the wrapped and unwrapped channel section of 100 mm web length and with the interior lip. The load-displacement curve at the initial loading was observed to be identical for both unwrapped and wrapped specimens. However, the load to failure for the latex wrapped section is increased to 4.8 kN.

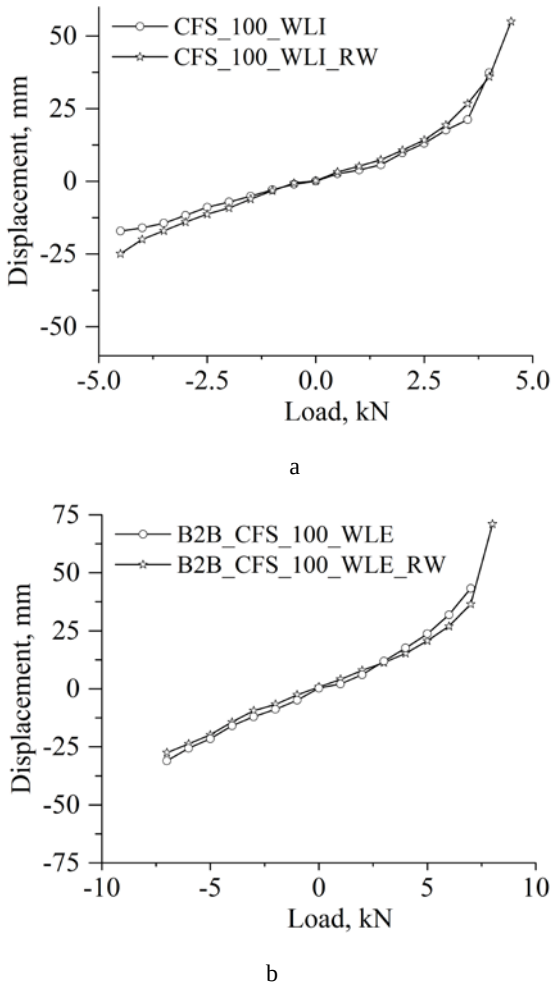

Fig. 7. Influence of latex wrapping on the load-displacement trend: a – channel section; b – back-to-back channel section

This is a 47 % increase when compared to the unwrapped section. A similar comparison of unwrapped and wrapped specimens for the back-to-back channel sections with exterior lip is shown in Fig. 7 b. The load-displacement curve at the initial cycle remained the same for both cases. The peak load to failure for latex wrapped

specimens increased by nearly 64 %. Some of the previous investigations have shown the wrapping of the CFS column with carbon fiber reinforced polymer (CFRB) and glass fiber reinforced polymer (GFRB) has increased the ultimate load to failure [23 – 25] during axial load testing. Chakaravarthy et al., 2022 [23], through experimental investigations showed that CFRP wrapped CFS column had improved the ultimate load by 1.66 times when compared to unwrapped CFS column. Another experimental investigation by Sreedhar et al., 2013 [24] on CFRP wrapped lipped channel section showed an increased ultimate capacity of up to 16.75 %. Sreedhar et al., 2013 [24] also highlighted that the bond between the CFRP-adhesive-steel is one of the governing factors in determining the strength of the member. Gao et al., 2013 [25] showed that the magnitude of increase in strength and stiffness due to the wrapping of CFRP member depends on the number of CFRP layers used. The current investigation is one of the first attempt to understand the influence of latex wrapping in CFS columns. From the experimental investigation, latex wrapping considerably increased the ultimate load during lateral loading of the CFS column.

To conclude, the lateral load-displacement curve was found to depend on the cross-section of the specimens. An increase in web length reduced the displacement of the specimen at any given load. The load-displacement curve for any cycle of loading for the section with and without a lip remained unchanged. Likewise, the load-displacement curve for initial cycles remained unchanged in both latex wrapped and unwrapped columns. However, the load to failure increases in the case of latex wrapped sections. Further, the strain recorded in the local buckling section is analyzed in the following section.

3.2. Ductility factor, energy absorption and stiffness of CFS column

The energy absorption was calculated for the ultimate load cycles and the influence of latex wrapping is studied. The area enclosed by the load-displacement plot indicates energy absorption. Fig. 8 shows the energy absorption of the selected samples and the energy absorption of all the samples tested are listed in Table 2.

Table 2. Energy absorption for all the specimens tested

No.	Sample	Energy absorption of unwrapped section, kN-mm	Energy absorption of latex wrapped section, kN-mm
1	CFS_100_NL	22.00	39.78
2	CFS_100_WLE	78.05	141.77
3	CFS_100_WLI	77.00	142.20
4	CFS_200_NL	104.90	175.20
5	CFS_200_WLE	145.05	174.80
6	CFS_200_WLI	169.15	206.20
7	B2B_CFS_100_NL	171.25	249.00
8	B2B_CFS_100_WLI	182.45	284.62
9	B2B_CFS_100_WLE	189.40	284.10
10	B2B_CFS_200_NL	207.30	335.55
11	B2B_CFS_200_WLE	227.40	325.28
12	B2B_CFS_200_WLI	211.50	317.20

Latex wrapping is said to increase the energy absorption in the specimen. The percent increase was found to vary with the column cross-section and provision of the lip. The energy absorption is found to increase approximately by 20 to 80 %. Table 3 shows the ductility factor for the specimens tested.

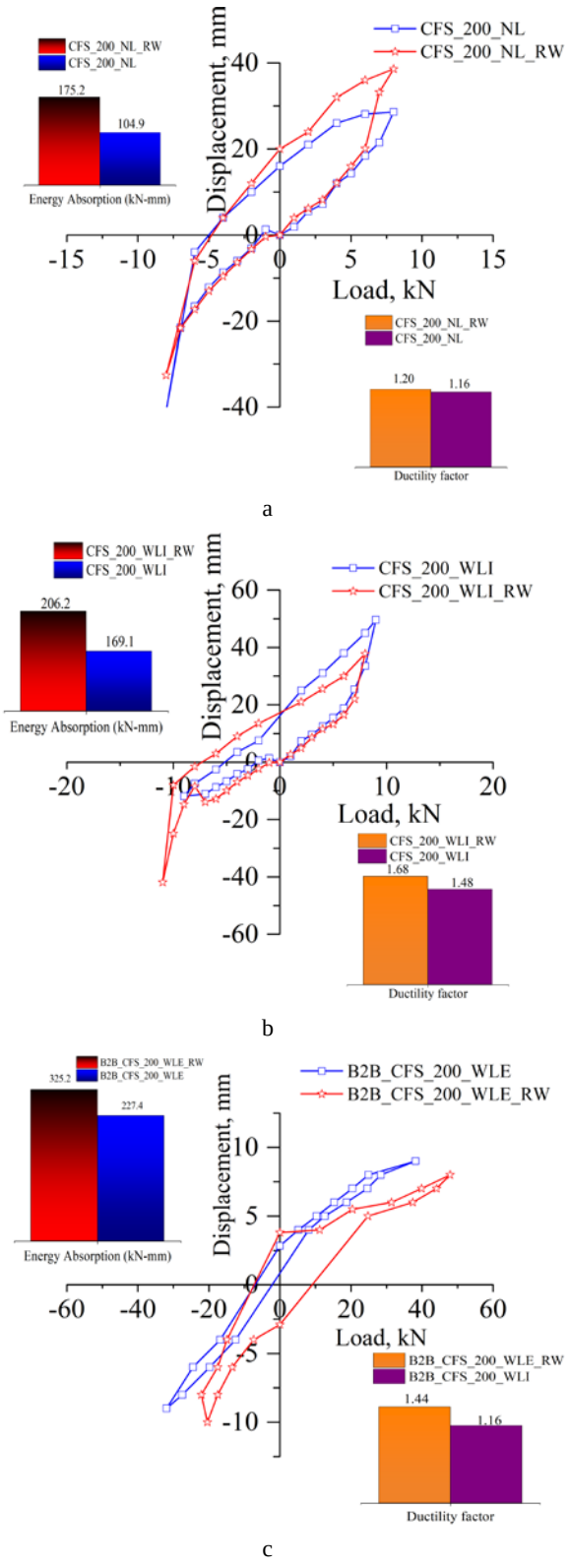

Fig. 8. Energy absorption and ductility factor for the CFS column specimens: a – CFS_200_NL; b – CFS_200_WLI; c – B2B_CFS_200_WLE

The ductility ratio is defined as the ratio of ultimate displacement to yield displacement. The ductility ratio was

found to be higher in latex wrapped samples. Fig. 9 shows the stiffness due to repeated loading for selected samples. Latex Wrapping increased the stiffness of the column. The increase in energy absorption and stiffness due to wrapping results are in line with the research finding of Gao et al., 2013, Sun et al., 2022 and Palanivelu et al., 2011 [25 – 27] reported for CFRP and GFRP wrapped CFS column section. Gao et al., 2013 [25] showed that a number of layers of CFRP wrapping influenced the stiffness and the wrapped sections exhibited 25 to 105 % increase in stiffness. Sun et al., 2022 [26] recommended GFRB wrapped CFS column for energy absorption structure due to its high energy absorption when compared to unwrapped section. The energy absorption capacity was found to depend on the cross-section geometry of the column [26, 27]. The current study showed that wrapping of CFS column with naturally available latex also increases energy absorption and stiffness.

Table 3. Ultimate displacement, yield displacement and Ductility factor for the CFS column specimens

No.	Samples	Displacement, mm		Ductility factor
		Ultimate	Yield	
1	CFS200-WLI-RW	41.9	24.9	1.68
2	CFS200-WLI	49.6	33.5	1.48
3	CFS200-WLE-RW	47.9	25.3	1.89
4	CFS200-WLE	38.2	28.6	1.34
5	CFS200-NL-RW	28.6	23.8	1.20
6	CFS200-NL	38.6	33.2	1.16
7	B2B-CFS200 –WLI-RW	62.1	27.0	2.30
8	B2B-CFS200-WLI	80.6	38.3	2.10
9	B2B-CFS-200-WLE-RW	83.7	58.2	1.44
10	B2B-CFS-200-WLE	53.4	46.0	1.16
11	B2B-CFS200-NL-RW	50.0	31.6	1.58
12	B2B-CFS-200 –NL	40.2	30.8	1.31
13	B2B-CFS100 -WLE-RW	31.0	15.9	1.95
14	B2B-CFS100 –WLE	34.7	28.8	1.20
15	B2B-CFS-100-WLI-RW	34.7	28.8	1.20
16	B2B-CFS100 –WLI	24.2	20.1	1.20
17	B2B-CFS-100-NL-RW	36.4	18.9	1.93
18	B2B-CFS-100-NL	23.5	13.8	1.70
19	CFS100-WLI-RW	24.9	20.0	1.25
20	CFS100-WLI	17.1	14.4	1.19
22	CFSC100-WLE-RW	36.4	18.9	1.93
21	CFSC100-WLE	46.6	25.5	1.83
23	CFS100-NL-RW	27.5	9.4	2.93
24	CFS100-NL	34.7	21.2	1.64

3.3. Strain at the local buckling zone

The variation in the strain at the depth of 100 mm from the base plate at different locations was analyzed. The strain gauges were fixed in the web, flange, and lip of the cross-section as shown schematically in Fig. 2. On comparing the strain measured at different locations, the strain recorded in the flange and the web was found to be critical when compared to the strain at the lip. Fig. 10 a shows the strain recorded at flange (point 2) and web (point 3) for CFS200_WLI. The strain in the flange reached maximum value before the web and the critical zone is observed to be the flange zone. This is seen in Fig. 10 b for CFS200_WLI and the same trend was observed for all the samples tested. For further analysis, the strain in the flange was used.

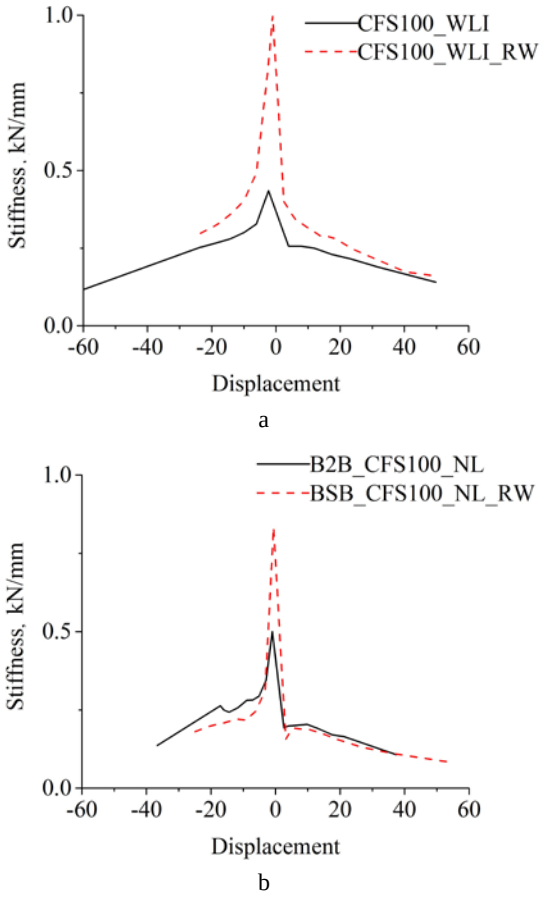

Fig. 9. Stiffness due to repeated loading for selected specimen: a – CFC 100_WLI; b – B2B_CFC_100_NL

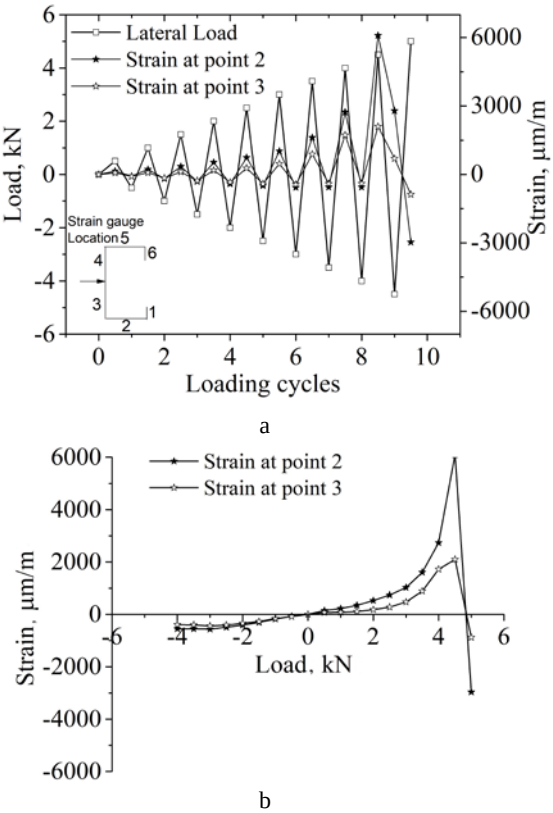

Fig. 10. Strain at different locations of specimen CFS200_WLI: a – load and strain variation with load cycles; b – lateral load ss strain

Fig. 11 compares the flange strain of the unwrapped channel section with the interior and exterior lip. Fig. 11 a shows the repeated cycles of load and strain and Fig. 11 b shows the peak strain in the respective section. The strain in the specimen with the interior and the exterior lip are observed to be opposite. This shows the inward and outward buckling nature of the interior lip and exterior lip section.

This observation also coincides with the type of failure observed in the failed samples. Fig. 12 shows the images of all the tested samples with a web length of 200 mm. All the specimens failed due to local buckling. The channel section with an interior lip and no lip exhibited similar damage.

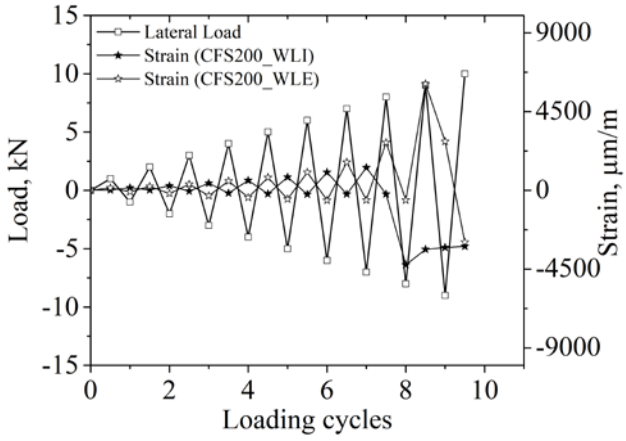

a

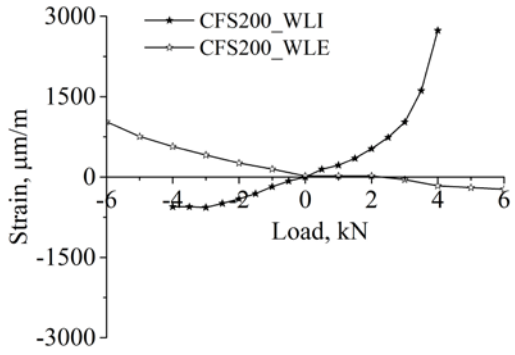

b

Fig. 11. Flange strain of channel section with interior and exterior lip: a – repeated load and strain; b – peak strain vs load

The flange in the section buckled inward as seen in Fig. 12 a and b. All the channel sections with exterior lip buckled outward as shown in Fig. 12 c. This leads to the opposite sign convention for the strain that is shown in Fig. 11. All the back-to-back channel sections with exterior lips and without lips exhibited outward buckling. This is shown in Fig. 12 d and f. All the back-to-back channel sections with interior lips exhibited inward buckling as shown in Fig. 12 f.

Fig. 13 shows the repeated loading and the corresponding strain response of the unwrapped and latex wrapped channel section with the interior lip. The ultimate load to failure of the unwrapped section is 6.6 kN and that of the wrapped section is 8 kN.

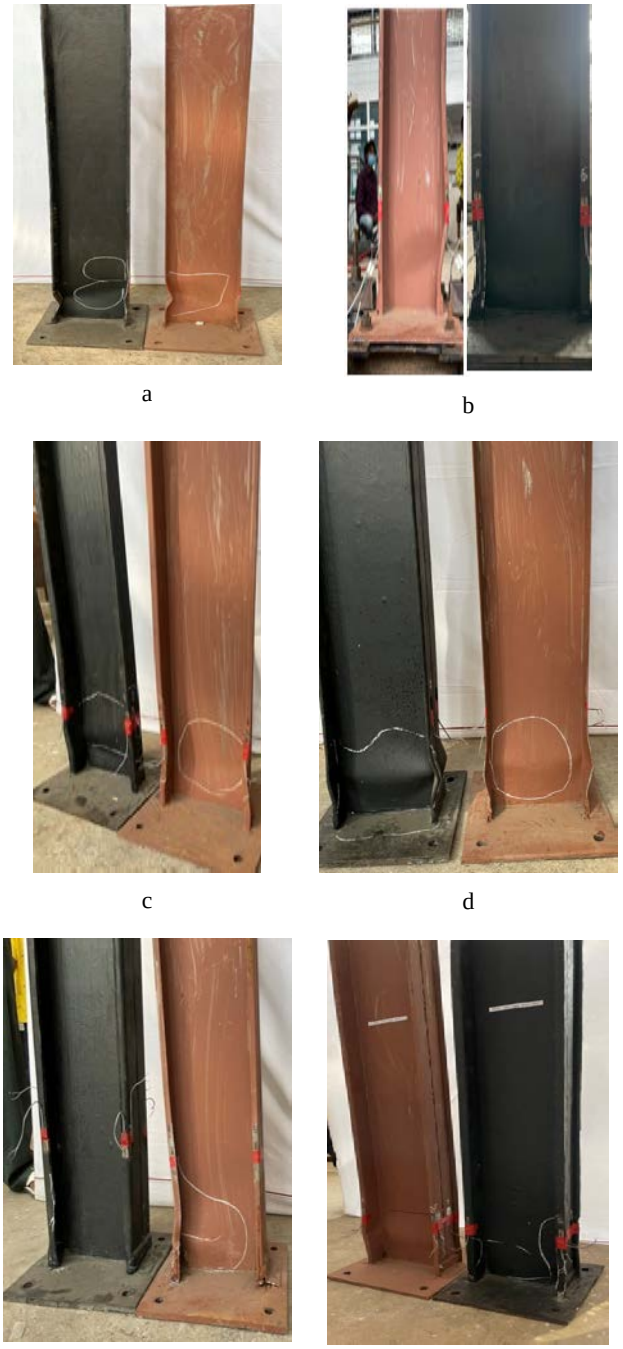

a b c d e f

Fig. 12. Images of the failed specimens: a – CFS_200_NL and CFS_200_NL_RW; b – CFS_200_WLI and CFS_200_WLI_RW; c – CFS_200_WLE and CFS_200_WLE_RW; d – B2B_CFS_200_NL and B2B_CFS_200_NL_RW; e – B2B_CFS_200_WLI and B2B_CFS_200_WLI_RW; f – B2B_CFS_200_WLE and B2B_CFS_200_WLE_RW

The corresponding strains are 4379 and 5270 mm/m. In this case, the latex wrapping increased the ultimate load to failure by 21 %. The corresponding strain also increased by about 20 %. Table 4 shows the ultimate load to failure and its corresponding strain for all samples tested. The ultimate load to buckling varied with the type of cross-section. On comparing the back-to-back channel section with its corresponding channel section, the lateral load to

failure increased by 70 to 120 %. In addition, there is a considerable reduction in the strain at the ultimate load point. The provision of interior or exterior lip also increased the ultimate load to buckling by 15 to 20 %. The latex wrapping increased the lateral load to failure by 15 to 25 %.

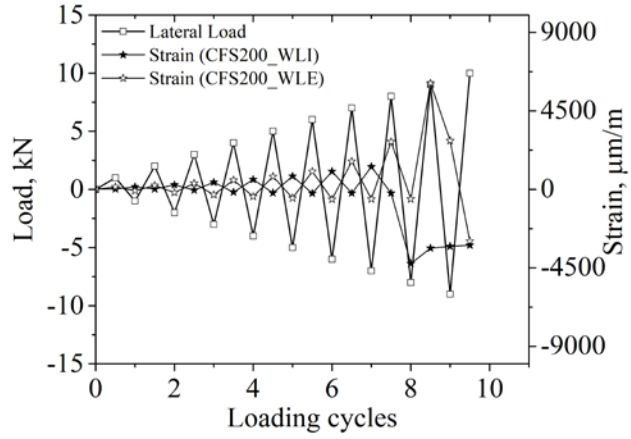

a

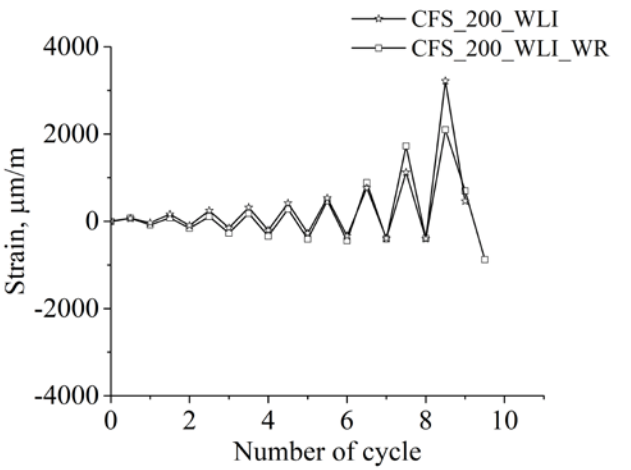

b

Fig. 13. Repeated load and the corresponding flange strain of the unwrapped and latex wrapped channel section with: a – load; b – strain

4. SUMMARY AND CONCLUSIONS

This paper reports the experimental investigation conducted to study the behaviour of various cold-formed steel cross-sections to repeated lateral loading. CFS columns were subjected to repeated lateral loading with incremental load magnitude for each loading cycle. The column was subjected to repeated loading till failure. All the columns were observed to fail in local buckling. Local buckling occurred near the base plate. The lateral displacement at the free end of the column and the strain in the local buckling zone were recorded and analyzed further to understand the behaviour of the column.

The strain in the flange zone was observed to be more critical in the local buckling zone. The damage was initiated from the flange portion. The increase in web length has a large influence on taking up the lateral load. The increase in web length of the column from 100 mm to 200 mm reduced the free end displacement by 30 to 40 % and the ultimate load to local buckling also increased by about 75 to 100 %.

Table 4. Ultimate load to failure and its corresponding strain

No.	Sample	Load, kN	Strain, μm/m
1	CFS_100_NL	3.5	6043
2	CFS_100_NL_RW	4.1	6850
3	CFS_100_WLI	4.0	6895
4	CFS_100_WLI_RW	4.8	7646
5	CFS_100_WLE	4.5	6062
6	CFS_100_WLE_RW	6.4	6613
7	CFS_200_NL	8.0	4738
8	CFS_200_NL_RW	9.4	5482
9	CFS_200_WLI	6.6	4379
10	CFS_200_WLI_RW	8.0	5279
11	CFS_200_WLE	6.4	4012
12	CFS_200_WLE_RW	8.0	4522
13	B2B_CFS_100_NL	8.0	6065
14	B2B_CFS_100_NL_RW	8.9	8516
15	B2B_CFS_100_WLI	8.2	6516
16	B2B_CFS_100_WLI_RW	9.0	8844
17	B2B_CFS_100_WLE	8.0	7628
18	B2B_CFS_100_WLE_RW	9.2	8249
19	B2B_CFS_200_NL	14.0	1390
20	B2B_CFS_200_NL_RW	14.8	2506
21	B2B_CFS_200_WLI	15.0	1094
22	B2B_CFS_200_WLI_RW	18.0	2260
23	B2B_CFS_200_WLE	18.0	2897
24	B2B_CFS_200_WLE_RW	19.0	3767

The provision of interior and exterior lips changed the type of local buckling that occurred in the flange portion of the cross-section. Flange buckled inward for the channel section without lip and with interior lip, whereas, the flange in the channel section with exterior lip buckled outward. The back-to-back channel section also exhibited buckling. The provision of lip (both interior and exterior) did not influence the load-displacement behaviour in both the free end and local buckling zone at the initial cycles of loading. However, increased ultimate load to failure was increased by 15 to 20 %. Energy absorption and ductility factor were calculated for all the samples tested and reported. The latex wrapping resulted in an increased energy absorption and it is about 20 to 80 % for different column cross sections. The ductility factor was found to be higher for latex wrapped samples as compared to unwrapped samples.

The wrapping of the column cross-section by natural latex did not influence the load-displacement behaviour at the initial cycles of loading. There is a marginal decrease in lateral displacement at failure observed near the free end of the column. Latex wrapping also increased the ultimate load to local buckling by 25 %. From the visible observation of the specimens after testing, some of the latex wrapped columns did not show buckling, however, while testing the load did not increase beyond a point. When the column is loaded, the major part of the load is transferred to the CFS section. With the natural latex being glued to the CFS column, the latex is expected to take the shape of the CFS column. On repeated loading, the column failed in local buckling but could not be visibly seen outside due to the swelling of latex in the local buckling zone. Further investigation on the latex wrapped section

considering it as a composite section and simulations to determine the effective thickness of the cross-section are in progress. Further, to implement the influence of wrapping to local buckling, one may need a different set of design equations [28].

REFERENCES

1. **Hancock, G.J.** Cold-Formed Steel Structures *Journal of Constructional Steel Research* 59 (4) 2003: pp. 473 – 487. https://doi.org/10.1016/S0143-974X(02)00103-7
2. **Hancock, G.J.** Cold-Formed Steel Structures: Research Review 2013–2014 *Advances in Structural Engineering* 19 (3) 2016: pp. 393 – 408. https://doi.org/10.1177/1369433216630145
3. **Schafer, B.W.** Cold-Formed Steel Structures Around the World: A Review of Recent Advances in Applications, Analysis and Design *Steel Construction* 4 (3) 2011: pp. 141 – 149. https://doi.org/10.1002/stco.201110019
4. **Usefi, N., Sharafi, P., Ronagh, H.** Numerical Models for Lateral Behaviour Analysis of Cold-Formed Steel Framed Walls: State of the Art, Evaluation and Challenges *Thin-Walled Structures* 138 2019: pp. 252 – 285. https://doi.org/10.1016/j.tws.2019.02.019
5. **Ye, J., Mojtabaei, S.M., Hajirasouliha, I.** Local-Flexural Interactive Buckling of Standard and Optimised Cold-Formed Steel Columns *Journal of Constructional Steel Research* 144 2018: pp. 106 – 118. https://doi.org/10.1016/j.jcsr.2018.01.012
6. CEN, EN. 1-3 Eurocode 3: Design of Steel Structures – Part 1-3: General Rules-Supplementary Rules for Cold-Formed Members and Sheeting. European Committee for Standardization, Brussels, 2006.
7. **Young, B., Rasmussen, K.J.R.** Behaviour of Cold-Formed Singly Symmetric Columns. *Thin-walled Structures* 33 (2) 1999: pp. 83 – 102. https://doi.org/10.1016/S0263-8231(98)00044-5
8. **Young, B., Rasmussen, K.J.R.** Shift of Effective Centroid of Channel Columns *Journal of Structural Engineering* 125 (5) 1999: pp. 524 – 531. https://doi.org/10.1061/(ASCE)0733-9445(1999)125:5(524)
9. **Young, B., Rasmussen, K.J.R.** Design of Lipped Channel Columns *Journal of Structural Engineering* 124 (2) 1999: pp. 524 – 531. https://doi.org/10.1061/(ASCE) 0733-9445(1998)124:2(140)
10. **Weng, C.C.** Effect of Residual Stress on Cold-Formed Steel Column Strength *Journal of Structural Engineering* 117 (6) 1991: pp. 1622 – 1640. https://doi.org/10.1061/(ASCE)0733-445(1991)117:6(1622)
11. Eurocode 3: Design of Steel Structures, Part 1–5: Plated Structural Elements, European Committee for Standardization, Brussels, 2005.
12. **Anbarasu, M., Kanagarasu, K., Sukumar, S.** Investigation on the Behaviour and Strength of Cold-Formed Steel Web Stiffened Built-up Battened Columns *Materials and Structures* 48 (12) 2015: pp. 4029 – 4038. http://dx.doi.org/10.1617/s11527-014-0463-8
13. **Kherbouche, S., Megnounif, A.** Numerical Study and Design of Thin-Walled Cold Formed Steel Built-up Open and Closed Section Columns *Engineering Structures* 179 2019: pp. 670 – 682. https://doi.org/10.1016/j.engstruct.2018.10.069
14. **Dar, M.A., Sahoo, D.R., Jain, A.K., Sharma, S.** Monotonic Tests and Numerical Validation of Cold-Formed Steel Battened Built-up Columns *Thin-Walled Structures* 159 2021: pp. 107275. http://dx.doi.org/10.1016/j.tws.2020.107275
15. **Naganathan, S., Chakravarthy, H.G., Anuar, N.A., Kalavagunta, S., Mustapha, K.N.B.** Behaviour of Cold Formed Steel Built-up Channel Columns Strengthened Using CFRP *International Journal of Steel Structures* 20 (2) 2020: pp. 415 – 424. http://dx.doi.org/10.1007/s13296-019-00293-5
16. **Dar, A.R.** Cold-formed Steel Composite Columns: Axial Strength and Deformation Response *Innovative Infrastructure Solutions* 6 (4) 2021: pp. 1 – 8. http://dx.doi.org /10.1007/s41062-021-00593-y
17. **Baabu, B.H., Sreenath, S.** Behaviour of Wrapped Cold-Formed Steel Columns Under Different Loading Conditions *In IOP Conference Series: Earth and Environmental Science* 80 (1) 2017: pp. 012025.
18. **Gajalakshmi, P., Jane Helena, H.** Behaviour of Concrete-Filled Steel Columns Subjected to Lateral Cyclic Loading *Journal of Constructional Steel Research* 75 2012: pp. 55 – 63. http://dx.doi.org/10.1016/j.jcsr.2012.03.006
19. **Ge, H., Usami, T.** Cyclic Tests of Concrete-Filled Steel Box Columns *Journal of Structural Engineering* 122 (10) 1996: pp. 1169 – 1177. http://dx.doi.org/10.1061/(ASCE) 0733-9445(1996)122(10)
20. **El-Taly, B.B.A., Fattouh, M.** Optimization of Cold-Formed Steel Channel Columns *International Journal of Civil Engineering* 18 (9) 2020: pp. 95 – 1008. http://dx.doi.org/10.1007/s40999-020-00514-7
21. **Imran, M., Mahendran, M., Keerthan, P.** Experimental and Numerical Investigations of CFRP Strengthened Short SHS Steel Columns *Engineering Structures* 175 2018: pp. 879 – 894. http://dx.doi.org/10.1016/j.engstruct.2018.08.042
22. **Shifferaw, Y., Schafer, B.W.** Cold-Formed Steel Lipped and Plain Angle Columns with Fixed Ends *Thin-walled Structures* 80 2014: pp. 142 – 152. http://dx.doi.org/10.1016/j.tws.2014.03.001
23. **Chakravarthy, N., Naganathan, S., Kalavagunta, S., Mustapha, K.N.B.** Structural Performance of Experimentally Investigated CFRP-Strengthened Cold-formed Steel Built-Up Columns *Iranian Journal of Science and Technology, Transactions of Civil Engineering* 46 (2) 2022: pp. 917 – 924. https://doi.org/10.1007/s40996-021-00706-8
24. **Kalavagunta, S., Naganathan, S., Mustapha, K.N.B.** Proposal for Design Rules of Axially Loaded CFRP Strengthened Cold Formed Lipped Channel Steel Sections *Thin-walled Structures* 72 2013: pp. 14 – 19. http://dx.doi.org/10.1016%2Fj.tws.2013.06.006
25. **Gao, X.Y., Balendra, T., Koh, C.G.** Buckling Strength of Slender Circular Tubular Steel Braces Strengthened by CFRP *Engineering Structures* 46 2013: pp. 547 – 556. http://dx.doi.org/10.1016/j.engstruct.2012.08.010
26. **Sun, G., Chen, D., Zhu, G., Li, Q.** Lightweight Hybrid Materials and Structures for Energy Absorption: A State-of-the-Art Review and Outlook *Thin-walled Structures* 172 2022: pp. 108760. http://doi.org/10.1016/j.tws.2021.108760
27. **Palanivelu, S., Van Paepegem, W., Degrieck, J., Vantomme, J., Kakogiannis, D., Van Ackeren, J., Hemelrijck, D., Wastiels, J.** Crushing and Energy

Absorption Performance of Different Geometrical Shapes of Small-Scale Glass/Polyester Composite Tubes Under Quasi-Static Loading Conditions *Composite structures* 93 (2) 2011: pp. 992 – 1007. https://doi.org/10.1016/j.compstruct.2010.06.021

28. **Mahar, A.M., Jayachandran, S.A., Mahendran, M.** Direct Strength Method for Cold-Formed Steel Unlipped Channel Columns Subject to Local Buckling *International Journal of Steel Structures* 21 (6) 2021: pp. 1977 – 1987. https://doi.org/10.1007/s13296-021-00547-1